



# Modeling and Analysis of Turbidity Currents in a Reservoir with the Dredged Guiding Channel

Nafeela Imtiyaz<sup>1a</sup>, Fong-Zuo Lee<sup>2b</sup>, Gwo-Fong Lin<sup>3c</sup>, and Jih-Sung Lai<sup>4d</sup>

<sup>a</sup>Hydrotech Research Institute, National Taiwan University, Taipei 10167, Taiwan (R.O.C.)

<sup>b</sup>Dept. of Civil Engineering, National Chung Hsing University, Taichung 40227, Taiwan (R.O.C.)

<sup>c</sup>Dept. of Civil Engineering, National Taiwan University, Taipei 10167, Taiwan (R.O.C.)

<sup>d</sup>Hydrotech Research Institute, Department of Bioenvironmental Systems Engineering, National Taiwan University, Taipei 10167, Taiwan (R.O.C.)

## ARTICLE HISTORY

Received 23 May 2023  
Revised 13 November 2023  
Accepted 20 March 2024  
Published Online 24 May 2024

## KEYWORDS

Reservoir sedimentation  
Turbidity current  
Reservoir management  
3D numerical model  
Venting efficiency  
Trapping efficiency

## ABSTRACT

Zengwen Reservoir, the largest water resource in Taiwan, has been seriously impacted by sedimentation, contributed mainly by typhoon floods. Therefore, it is chosen as a case study to investigate the effectiveness of an integrated reservoir management strategy of sediment routing and removal by constructing a dredged guiding channel to route turbidity currents generated during typhoon floods. The strategy is evaluated by simulating flood events of four return periods using a 3D numerical model, the effectiveness of which, with and without the dredged guiding channel, is compared in terms of the venting efficiency of reservoir outlets and the arrival time of turbidity currents. The numerical model is calibrated using the laboratory data and validated using the physical model and field data. The simulated results show a significant increase in the venting efficiency and a decrease in the arrival time of turbidity current for all the flood events in the presence of a dredged guiding channel. In addition, results also aid in predicting trapping efficiency based on the Brune curve trend for different capacity inflow ratios for single flood events. The findings demonstrate the feasibility and effectiveness of the integrated reservoir management strategy in the field before high-intensity flood events.

## 1. Introduction

The issue of reservoir sedimentation has caused significant problems in many parts of the world, resulting in severe implications for water conservation, flood control, and energy production. The global average loss of reservoir storage capacity due to sedimentation has been reported to range between 0.5 – 1% per annum (Mahmood, 1987; Wissler et al., 2013). The sediment settling phenomenon in the reservoir is influenced by various factors, including the hydrology of the catchments and the geological characteristics of the river basin. Sediment transport is naturally balanced in the streams with no obstruction. A structure like a dam disturbs this naturally developed balance. As the sediment-laden flow approaches the dam, its velocity decreases and causes sediment to settle. Even though highly beneficial in flood control and drought prevention, a dam eventually becomes a cause of

problems in a naturally balanced river ecosystem (Kondolf et al., 2019). Reservoir sedimentation can reduce the storage capacity of the reservoir and increase the possibility of blockage of intake structures, posing a threat to the functioning of the hydropower plant and other reservoir outlets (Morris and Fan, 2009). The categories of management strategy to address reservoir sedimentation are techniques, including reducing sediment inflow from the upstream watershed, routing sediment through the reservoir to minimize deposition, and removing sediment deposits (Morris and Fan, 2009; Lee et al., 2014; Annandale et al., 2016). However, techniques, i.e., reducing watershed sediment and demolishing the existing dam to restore the reservoir's storage capacity and sediment balance, may be neither cost-effective nor engineeringly feasible. Hence, researchers will need to devise better and more effective management strategies to provide sufficient reservoir storage to combat major floods and ensure the sustainability of reservoirs.

**CORRESPONDENCE** Fong-Zuo Lee ✉ [fzlee@nchu.edu.tw](mailto:fzlee@nchu.edu.tw) Dept. of Civil Engineering, National Chung Hsing University, Taichung 40227, Taiwan (R.O.C.)

© 2024 Korean Society of Civil Engineers

During flood events, a turbidity current may be generated in the reservoir. A turbidity current is a gravity-prompted movement of sediment-laden flow over, through, or under the ambient fluid caused by the density difference between the two fluids (Sastre et al., 2010). Turbidity current is a type of density current caused primarily by the presence of turbidity. This current occurs when sediment-laden flow plunges beneath the clear water as it enters an impoundment and travels along the bottom elevation or submerged thalweg towards the downstream. Turbidity currents generated during flood events can significantly impact sediment deposition in reservoirs. Therefore, turbidity currents must be adequately understood and analyzed to manage and operate hydraulic infrastructure sustainably and effectively. To avoid sedimentation in the critical locations of the reservoir, it becomes essential to understand the factors affecting the turbidity currents and reservoir sedimentation mitigation. For several decades, turbidity flows have been a topic of theoretical debate (Schleiss et al., 2016). Many studies have been done in the past to understand the factors influencing the controlled movement of turbidity currents (Oehy and Schleiss, 2007; Marosi et al., 2015). However, limited studies have focused on reservoir sediment management strategy, i.e., turbidity current venting through reservoir outlets and the influencing factors. The outlet's location plays a vital role in achieving optimum sediment venting. The sediment outflowing concentration of bottom outlets is higher than that of elevated outlets due to the stratification phenomenon of turbidity currents (Morris and Fan, 2009; Lee et al., 2014). However, it is also essential to understand the influence of the time of gate opening of these reservoir outlets. Chamoun et al. (2018) found that gates must be opened when the turbidity current is roughly 300 m upstream of the outlet to maximize the sediment outflow concentration. The bed slope also influences the venting of the turbidity currents (Morris and Fan, 2009). Higher venting efficiencies are attained when the thalweg upstream of the dam is steeper (Chamoun et al., 2017). According to the literature, research has yet to determine the influence of the integrated sediment management strategy of dredged guiding channel and sediment routing on the flood-induced turbidity currents inside the reservoir. However, observing and analyzing turbidity currents in the field is highly challenging, as they are typically generated during floods. Thus, in most cases, field observation and investigation are limited. Hence, simulating sediment movement in the reservoir using numerical models can help understand the phenomena of a turbidity current. Therefore, hydrodynamic and sediment transport modeling is essential for the analysis of the process of sedimentation in a reservoir. To study sediment-laden flow in a reservoir, the numerical models commonly employed may be based on solving the one-dimensional or the two-dimensional Saint-Venant equations. However, these models can reproduce reasonable results for many applications to provide accurate predictions, which need to be calibrated precisely. In regions where consideration of three-dimensional effect is crucial, i.e., strong vertical non-uniformity of the flow field exists, such cases must consider using the numerical models based on solving the 3D Navier-Stokes equations

that govern complex fluid flows and sediment concentrations. Among the 3D numerical models, the literature has employed solvers such as the CFX series to compute the two-phase flow parameters associated with turbidity current (De Cesare et al., 2001, 2006; Oehy and Schleiss, 2007; Lee et al., 2014; Amini et al., 2017; Jodeau et al., 2018). Therefore, the ANSYS-CFX is used in the present study to simulate turbidity current generated due to typhoon-induced floods with unsteady inflow conditions herein.

The changing climate patterns have made natural disasters like floods and droughts very imminent in the region of Taiwan. Taiwan receives 2,500 mm of yearly precipitation on average. Due to Taiwan's fragile geological and hydrological characteristics, a large amount of sediment flows into the reservoir from the watershed. Additionally, Taiwan's steep slopes have exacerbated the problem of reservoir sedimentation in several strategically vital areas, the watershed of Zengwen Reservoir being one such crucial region. Due to typhoon flood occurrences, turbidity currents are generated, and hence substantial sedimentation rates have been seen in the Zengwen Reservoir. Therefore, this study aims to find a sustainable solution that will help maximize the venting of the turbidity currents through reservoir outlets to maintain the uninterrupted functioning of the reservoir.

Based on the literature review above, the 3D numerical model ANSYS-CFX proves to be valuable and feasible for simulating turbidity currents in Zengwen Reservoir to analyze sediment concentration venting efficiency through reservoir outlets. Initially, experimental data from the laboratory flume are used for mesh analysis and parameter calibration of the 3D model. Subsequently, physical model data and field data from Zengwen Reservoir are collected to verify the accuracy of simulated sediment concentration and outlet venting efficiency. Notably, an innovative nature-based idea is proposed, integrating two techniques: sediment routing and removal. This idea aims to be achieved by constructing a dredged guiding channel to route turbidity currents through the reservoir. The effectiveness of this strategy, with and without the dredged channel, is compared in terms of outlet venting efficiency under various return-period flood conditions.

## 2. Description of Study Area and Hydrological Conditions

The Zengwen Dam, built in 1973, with a height of 134 m and a length of 400 m, is Taiwan's largest dam, impounding the largest reservoir by volume. It is located in the upper reach of the Zengwen River in southern Taiwan. The Zengwen Reservoir has a catchment area of 481 km<sup>2</sup>, as shown in Fig. 1(a). The reservoir has a maximum daily inflow volume of 340 Mm<sup>3</sup> ( $M = 10^6$ ) and an annual inflow volume of 1740 Mm<sup>3</sup>. The length of the reservoir pool from the dam site to the Dapu check dam is 15.1 km, the upstream barrier, with a normal water level of 230 m, forming a water surface area of 19.04 km<sup>2</sup>. As shown in Fig. 1(b), the outlets present in the reservoir are three spillways, a power plant intake, a bottom outlet, and a desilting tunnel with a design discharge of

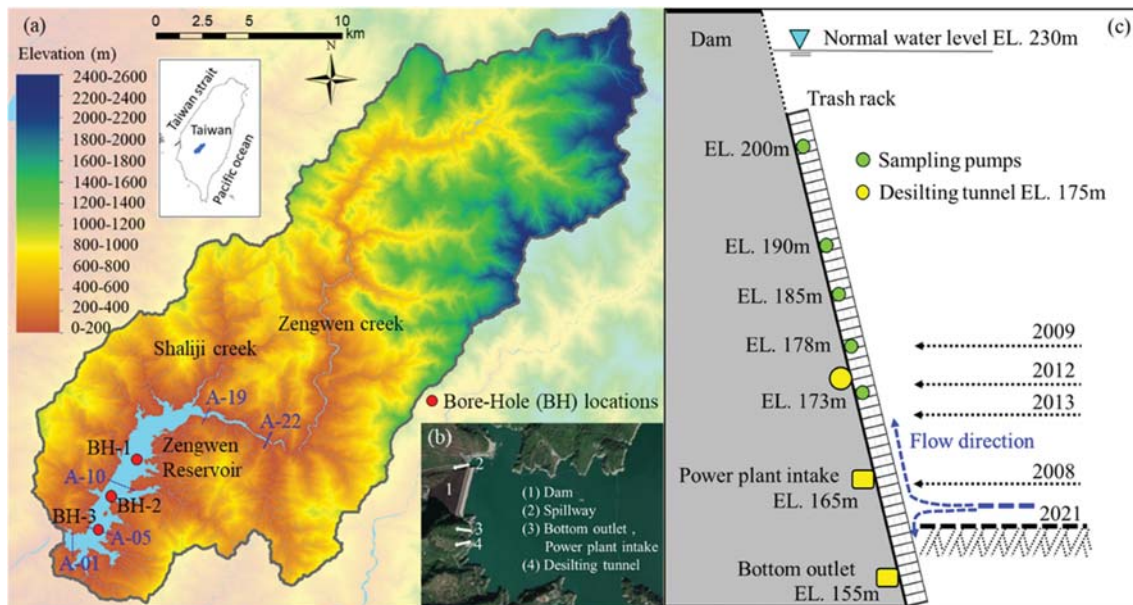


**Fig. 1.** Zengwen Reservoir Facilities (a) The Watershed of Zengwen Reservoir, (b) Location of Reservoir Outlets and Dam, (c) Illustration for the Cross-Sectional View of Intake Structure and Outlets

9,470 m<sup>3</sup>/sec, 56 m<sup>3</sup>/sec, 150 m<sup>3</sup>/sec and 995 m<sup>3</sup>/sec, respectively. In the cross-sectional view, the positions of the intake, outlets, and sediment sampling pumps are illustrated in Fig. 1(c). The Zengwen Reservoir is a multi-purpose reservoir that serves irrigation, municipal, industrial, hydropower generation, recreation, and flood control demand. However, the primary function is to supply water to the irrigation system of region 854.24 km<sup>2</sup> in the Chianan Plain, an essential food production area in Taiwan (Wang et al., 2018).

The on-site geological drilling and soil test report by the Southern Region Water Resources Office, Taiwan, has been referred to gain insight into the sediment particle size within the reservoir. According to the report, three bore-hole (BH) locations were chosen to evaluate the particle size analysis in the Zengwen Reservoir (as shown in Fig. 1(a)), BH-1 (cross-section between A12 and A13), BH-2 (cross-section A9), and BH-3 (cross-section A5).

At each BH, ten samples were collected at different depths ranging from 1.05 – 15 m. The report results suggest that particle size variation along depth was more significant at BH-03 than at BH-01 and BH-02. Also, the percentage of silt and clay was higher at BH-01 and BH-02. It reveals that the turbidity current consisting of silt and clay gets transported to the reservoir outlets (Southern Region Water Resources Office, 2021a). In addition, based on the report of the sediment concentration monitoring project, it was found that the sediment sampled at the dam site (as shown in Fig. 1(c)) had the mean particle diameter size  $d_{50} = 5.6 \mu\text{m}$  after a torrential rainstorm and Typhoon Saola in 2012.

Taiwan is known for producing the most significant amount of sediment worldwide owing to its steep topography, frequent tectonic activity, fragile geology, intense precipitation, and frequent floods (Dadson et al., 2003). The Zengwen Reservoir receives a

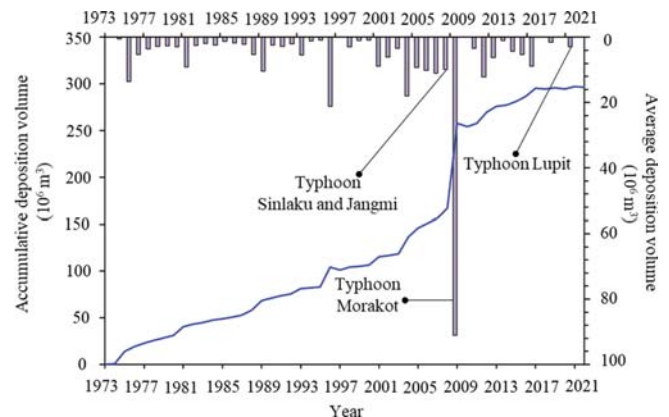


**Fig. 2.** Historical Sedimentation Record in Zengwen Reservoir

large amount of sediment yield due to the torrential rains (Wu et al., 2021). However, typhoon-induced landslides are the primary cause of sedimentation in the Zengwen reservoir. Fig. 2 shows the sedimentation data of accumulated and average annual deposition volumes over the years in the Zengwen Reservoir. In 2022, the accumulative deposition volume reached 295.4 Mm<sup>3</sup>. However, with an existing storage capacity of 453 Mm<sup>3</sup>, the estimated storage capacity of the Zengwen reservoir was 60.53% of its initial capacity. Impacted by typhoon flood events, it has experienced significant sediment yields from its upstream watershed over the past few decades. Among typhoon events, Typhoon Morakot was the most destructive tropical typhoon that hit Taiwan from August 7 to 9, 2009. The prolonged movement of Typhoon Morakot during both the landfall and post-landfall phases contributed to the heavy rainfall. It poured 2,550 mm average rain in the Zengwen Reservoir watershed, generating 1467 hectares of landslides. As a result, the reservoir's capacity was reduced by

91.08 Mm<sup>3</sup> (13 percent of its initial capacity). Also, a massive amount of sediment and debris had deposited surrounding the reservoir outlets, disrupting the functioning of the reservoir. The reservoir bed accumulated sediment up to EL. 179.1 m, substantially higher than the intake's invert elevation (EL. 155 m), causing the bottom outlet to malfunction (Wang et al., 2018).

Since 2012, structural changes have been performed, including refurbishment of the bottom outlet, construction of maintenance tunnels, and a desilting tunnel to increase the sediment outflow through the outlets. Additionally, to restore the lost capacity and remove the sediment deposits near the outlets, a dredging operation was started in December 2012. It was the first dredging operation since the dam construction in 1973. During dredging, the covered area was in the fan shape with a radius of 600 m and an angle of 120 degrees extending from the reservoir's intake gatehouse. The total dredged volume from 2012 to 2018 was 4.06 Mm<sup>3</sup>. Further dredging was continued to the distance of 1,000 m starting from the dam site, and the amount dredged from 2019 to 2022 was 10.68 Mm<sup>3</sup>.

However, with the anticipated average annual inflow sediment of 5.06 Mm<sup>3</sup>, it is clear that yearly dredging near the intake will not be able to sustain reservoir capacity. As mentioned earlier, integrating various reservoir management strategies by different techniques to deal with flood-induced turbidity currents is crucial to reduce sedimentation problems. Combining sediment routing and dredging techniques aims to increase the venting efficiency by constructing a dredged channel guiding and routing turbidity current through the reservoir. A two-dimensional (2D) layer-averaged model developed by Lai et al. (2015) was adopted to simulate turbidity current venting through reservoir outlets (Lai et al., 2015; Huang et al., 2019). A preliminary study using this 2D model was adopted to evaluate the effect on venting efficiency by selecting various widths, lengths, and depths of the dredged channel. It was found that considering the width of 200 m and the depth of 5 m was a workable dimension for the field operation with more effective venting benefits in Zengwen Reservoir (Southern Region Water Resources Office, 2021b). Therefore, in the present study, using the 3D numerical model we construct a dredged channel extending from cross-section A-01 to cross-section A-10, 200 m wide and 5 m deep, to simulate the turbidity current venting through reservoir outlets.

### 3. Methodology

#### 3.1 Numerical Model

The reservoir turbidity currents are simulated using ANSYS-CFX as a 3D model. There are liquid and solid phases in the currents, and it is a two-phase problem involving a water-sediment mixture. Most of the sediments transported to the dam are silt and clay, with small particle sizes in the study site. Flow can be considered a single-phase fluid if the collisions between sediment particles and the momentum changes between the water and the sediments are ignored. Suppose we assume water and sediments of turbidity current as a single entity. In that case,

we may use the algebraic slip model's analog notion to simplify multiphase flow equations into a single-fluid equation for addressing flow conditions with small particles of sediment-laden flow (De Cesare et al., 2001; Oehy and Schleiss, 2007). The sediment relaxation time of small particles is assumed to be substantially shorter than the calculated time of the total flow in the model. It signifies that the particle dispersion volume fraction is exceedingly small. As a result, using the momentum equation to solve the particle motion state is unnecessary. In addition, the data from flume experiments and physical model tests are collected for parameter sensitivity analysis and to verify the capability of the 3D numerical model in simulating turbidity current movement.

#### 3.1.1 Model Description

3D-based Computational Fluid Dynamics (CFD) codes are employed to achieve highly accurate numerical solutions for challenging field topography such as of a reservoir and desilting outlets. The ANSYS, Inc. issued solver CFX enables the execution of user code and expert commands (De Cesare et al., 2001; Oehy and Schleiss, 2007; Chamoun et al., 2017). Suspended sediment concentration is included in the CFX formulas through its advection-diffusion model with a continuous and homogeneous Eulerian description. Solving mass balances of turbid water and momentum balance for the mixture accounts for the changing mixture density are considered on different mass fractions. The transfer of mass and momentum from one phase to another is not considered. The k-epsilon turbulence model is used to calculate the turbulent stresses, which employs the eddy-viscosity hypothesis to introduce the momentum transportation of turbidity current. The method is isothermal and incompressible, indicating no heat transfer is considered, and hence no thermal energy balance is solved. The buoyancy effect is adapted through variable parameters. The fluid density is defined by the sediment mass fraction concentration, with the Reynolds-averaged Navier-Stokes equations serving as the basis for the computation. In this study, we also take the fall velocity of the particles into account. The continuity equation Eq. (1) and the momentum equation Eq. (2), along with Eq. (3) for sediment concentration, are the governing equations for turbidity current movement.

$$\frac{\partial \rho}{\partial t} + \frac{\partial}{\partial x_i} (\rho U_i) = 0, \quad (1)$$

$$\frac{\partial (\rho U_i)}{\partial t} + \frac{\partial (\rho U_i U_j)}{\partial x_j} = -\frac{\partial p'}{\partial x_i} + \frac{\partial}{\partial x_j} \left[ \nu_{eff} \left( \frac{\partial U_i}{\partial x_j} + \frac{\partial U_j}{\partial x_i} \right) \right] + G'_i - w_f w_j \frac{\partial}{\partial x_i} \left( \frac{\rho_w \rho_s}{\rho} \right), \quad (2)$$

$$\frac{\partial (\rho c_p)}{\partial t} + \frac{\partial (\rho c_p U_i)}{\partial x_i} = \frac{\nu_{eff}}{\sigma_p} c_p \left( \frac{\partial U_i}{\partial x_j} + \frac{\partial U_j}{\partial x_i} \right) - w_f \frac{\partial}{\partial x_i} \left( c_p \frac{\rho_w}{\rho} \right), \quad (3)$$

where  $\rho$  = mixture density =  $(1 - c_p)\rho_w + c_p\rho_s$ ;  $c_p$  = sediment particle concentration;  $\rho_w$  = water density;  $\rho_s$  = particle density,  $t$  = time;  $x_{ij}$  = cartesian coordinates  $\equiv (x, y, z)$ ;  $U_{ij}$  = velocity components  $\equiv (u, v, w)$ ;  $p'$  = modified pressure;  $\nu_{eff}$  = effective viscosity;  $G'_i = [0, 0, (\rho - \rho_w)g]$  is a buoyancy vector;  $w_f$  = fall velocity of a sediment particle;  $g$  = acceleration due to gravity, and  $\sigma_p =$

turbulent Prandtl number for the sediment concentration.

Based on the eddy viscosity concept,  $\nu_{eff}$  is similar to the zero-equation model as  $\nu_{eff} = \nu + \nu_t$ ; where  $\nu$  is the kinematic viscosity of water and  $\nu_t$  is the turbulence viscosity. The turbulence viscosity is linked to the turbulence kinetic energy and dissipation via following relation  $\nu_t = C_v \rho k / \varepsilon$ ; where  $C_v = 0.09$  is a constant  $k$  is turbulent kinetic energy, and  $\varepsilon$  is turbulence dissipation rate. In addition, we also considered  $\nu_{eff}$  of the mixture by employing Van Rijn's (1987) equation for the kinematic viscosity of a sediment-laden flow. Then, we employed a concept earlier used by Chamoun et al. (2018) to decide on effective viscosity as Eq. (4) using viscosity and sediment concentration.

$$\nu_{eff} = \min(\nu(1 + \lambda)(1 + 0.5\lambda), 5, \nu + \nu_t), \quad (4)$$

where  $\lambda$  is used to develop a relationship between concentration and mixture viscosity as Eq. (5).

$$\lambda = ((a / (0.7399c_p + 0.0001))^{1/3} - 1)^{-1}, \quad (5)$$

where  $a$  is a viscosity coefficient.

Regarding the fall velocity of a particle, Morris and Fan, (2009) was the first to provide a formula for calculating the fall velocities of gravel, sand, and silt particle. Many researchers have proposed a variety of semi-theoretical and empirical relationships for the fall velocity since then (Morris and Fan, 2009). In this study, the fall velocity  $w_f$  in water with suspended sediment concentration  $c_p$  can be estimated using the equation proposed by Richardson and Richardson and Zaki (1954) in Eq. (6).

$$w_f = w_{tf}(1 - c_p)^m, \quad (6)$$

where  $w_{tf}$  is the terminal fall velocity of a particle in clear water, and  $m$  is a Reynolds number (Re) dependent coefficient. Camenen (2007) and Zhiyao et al. (2008) proposed an equation for  $w_{tf}$  in clear water. It can be expressed as a function of sediment particle diameter in the following formula.

$$w_{tf} = \frac{\nu}{d} d_*^3 \left( 38.1 + 0.93 d_*^{\frac{12}{7}} \right)^{\frac{7}{8}}, \quad (7)$$

where  $d_* = (\Delta g / \nu^2)^{1/3} d$ ;  $d$  is the particle diameter and  $\Delta = \rho_s / \rho - 1$ .

Regarding  $m$ , the values range from the least of 2.25 to the highest value of 7. Richardson and Zaki (1954) proposed  $m = 4.65$  for laminar flow, and  $m = 2.39$  for  $Re > 500$ ; however, as summarized by Chien and Wan (1999), several  $m$  values ranging from 1 to 7 have been proposed over the past decades in which  $m$  values depend on the medium diameter of the particle as well. In this study, the additional CFX Command Language (CCL) function of the inflow discharge or velocity distribution and volumetric fraction were programmed as Dirichlet type into the boundary setting. The outlet flux was established in accordance with the experimental model and field operation.

## 4. Results and Discussion

The data used in this study includes flume experiment data

generated in the laboratory for numerical model calibration (Lee, 2013). In addition, the physical model data obtained from the Water Resources Planning Institute (2018) were used to verify the accuracy of simulated turbidity current arrival time and venting efficiency for bottom outlets. Further, field data were obtained from Zengwen Reservoir from the Southern Region Water Resources Office (2021b) for model validation to corroborate that the calibrated parameters are unaffected by the scale effect between the laboratory test, model scale test, and the field.

### 4.1 Turbidity Current Venting Simulations Using Laboratory Data for Model Calibration

Numerical model geometry was constructed similarly to the flume used for the experiments by Lee (2013). The data from the experiment conducted in a 1 m long, 0.05 m wide, and 0.35 m deep glass-walled flume was used to calibrate the numerical model. The experiments were conducted previously to understand the stratification effect in turbidity current and location effect on sediment desilting through reservoir outlet. The slope of the flume bottom was adjustable and set to be horizontal. A head tank with a mechanical stirrer was equipped to keep inflow sediment particles homogeneous in suspension. The suspended sediment mixture was supplied to the upstream end of the flume by controlling the valve, which created the sediment-laden flow moving toward the downstream outlet. At the end wall of the flume, a bottom outlet dimension of 0.05 m in width and 0.002 m in height was installed and controlled by valves. To maintain steady water surface elevation, an excessive water supply without disturbing the flow field was drained through an overflow weir at the downstream end of the flume. For mesh analysis, five simulation mesh sizes were tested; the mesh size equal to 1/10 of the bottom outlet diameter reveals sufficient accuracy and consumes less CPU time. Therefore, the referenced computational mesh of 1/10 outlet diameter is adapted for the following model calibration and application cases. In addition, the grid size also referred to the suggestion of Lee et al. (2014) to ensure simulated accuracy. The simulation mesh of a flume is hexahedral throughout the geometry and comprises 23,100 nodes and 17,928 elements. The mesh is made denser by opting for inflation near the region close to the bed and the outlet since it's essential to analyze the turbidity currents.

The inflow boundary condition set as Dirichlet type was given by a vertical distribution of unit width discharge and sediment concentration at the inlet. The maximum inflow concentrations are given as 7000 ppm (case 1) and 9000 ppm (case 2). The sediment material with mean particle diameter size  $d_{50} = 5.6 \mu\text{m}$  is used in the experiment, which was collected and sampled from the Zengwen Reservoir. The overflow weir was set at a zero normal velocity gradient and hydrostatic pressure distribution, whereas the bottom outlets were set for measured outflow discharges. A no-slip boundary condition was set for walls and bed, whereas rigid-lid approximation was established as a boundary condition for the water surface, implying that the initial surface atmosphere pressure was set to zero and that the free surface was regarded as

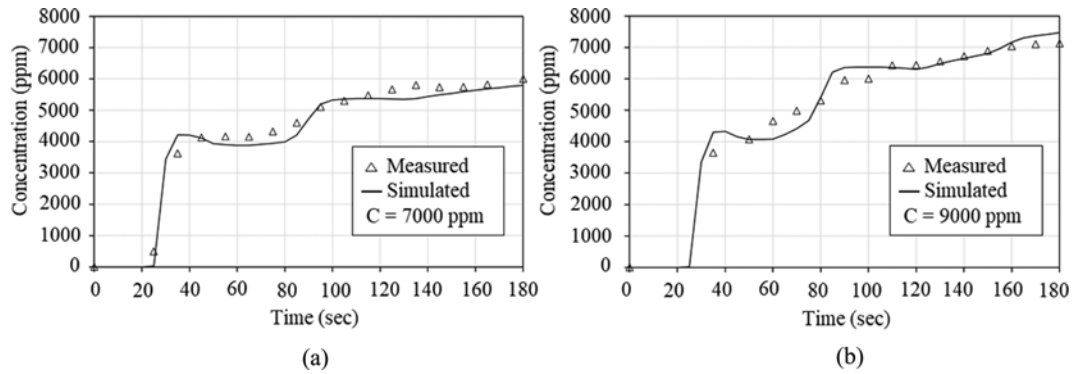


Fig. 3. Sediment Outflow Concentration Through the Outlet Under: (a) Inflow Concentration is 7000 ppm, (b) Inflow Concentration is 9000 ppm

a symmetry surface for all variables (De Cesare et al., 2006; Lee et al., 2014). The sediment concentration and fluid velocity are set to zero for the initial state of the flume. To calibrate the parameter of viscosity coefficient ( $a$ ) in Eq. (5), different values for coefficient  $a$  ranging from 0.5 to 3.0 were tested, and  $a$  value of 1 showed the least deviation. The calibrated values of coefficient  $a$  in this study are close to the previous research value, 0.67, reviewed by Van Rijn (1987) and Sabine Chamoun et al. (2018). Further sensitivity analysis revealed that coefficient  $m$  of Eq. (6) had a limited influence on the outcome under the present simulations, and fine sediment dominated the turbidity current movement. In addition, the value of  $m$  is considered 4.65 for fine sediments by Lee et al. (2014). Hence,  $m$  was given a value of 4.65 in this study.

From the simulated results, the turbidity current arrives at the bottom outlet first due to the stratification of the suspension in clear water. In addition, when compared with the measured results, the simulated results show consistency and follow the trend. Fig. 3 indicates that the simulated outflow concentrations obtained using the k-epsilon turbulence model fit well with experimental measurements, with a standard error of 3.02 percent and 0.80 percent for case 1 and case 2 from measured data, respectively. Furthermore, it reveals that the adapted k-epsilon turbulence model has high convergence and requires less memory.

#### 4.2 Turbidity Current Simulation Using Physical Model Data for Verification

The Zengwen Reservoir was severely silted due to heavy rains from Typhoon Morakot in 2009. In addition, the increase in sedimentation in the reservoir alarmed a crucial need for effective reservoir management techniques. Hence, a plan for managing sediment in Zengwen Reservoir was issued to make sustainable use of water resources, including constructing a desilting tunnel. The physical model of Zengwen Reservoir with a model scale ratio of 1:100 was constructed, and tests were conducted to evaluate the venting efficiency at the existing outlets and the planned desilting tunnel (Water Resources Planning Institute, 2018). Experimental data of turbidity current movement and outflow concentration at the outlets were used to verify the numerical model.

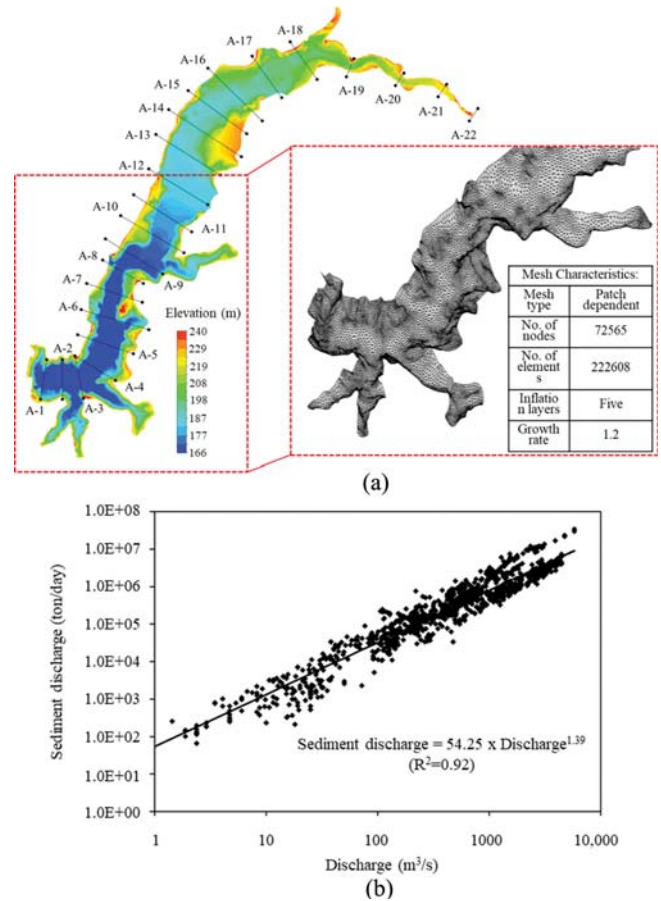
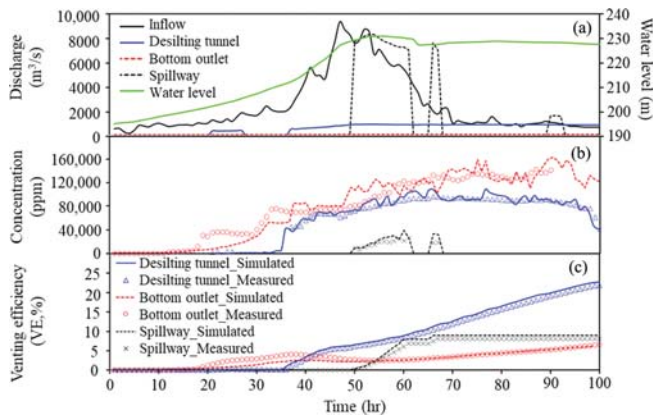


Fig. 4. The Simulation: (a) Domain with Cross Sections and Meshes, (b) Relationship between Sediment Discharge and Inflow Discharge

A simulation domain encompassing the site of interest contains 22 surveyed cross-sections from the Zengwen Dam to cross-section A-22 near Dapu hydrological station, about 15.1 km. For the upstream boundary, the field-measured data of inflow discharges and sediment concentrations at the Dapu hydrological station were provided as the boundary conditions. The spillway, desilting tunnel, and bottom outlet were the three downstream outlet boundaries in modeling. A 3D mesh using tetrahedral cells with 222,608 elements and 72,565 nodes covers the



**Fig. 5.** In the Typhoon Morakot Event, the Hydrographs of: (a) Discharge and Water Level, (b) Simulated and Measured Concentration, (c) Simulated and Measured Venting Efficiency Through Various Outlets

simulation domain, as shown in Fig. 4(a). The inflow sediment concentration is obtained using the relationship plotted in Fig. 4(b).

The inflow discharge and sediment concentration hydrographs at the Dapu station are used as the inlet boundary conditions. The flood event during Typhoon Morakot was selected as the study case in the physical model and hence used for model verification as well. Under the hydrological conditions of Typhoon Morakot, data recorded include water level, inflow discharge, and outflow discharge, as shown in Fig. 5(a). The outflow discharge hydrographs of the reservoir outlets are used as the outflow boundary conditions, also shown in Fig. 5(a). The inflow peak discharge occurred at 47 hr. and reached 11,729 m<sup>3</sup>/sec. Based on the arrival time of the turbidity current reaching the dam, the gates of the desilting tunnel and bottom outlet were opened to vent the turbidity current. The designed discharge capacity of the desilting tunnel and bottom outlet is 995 and 150 m<sup>3</sup>/sec, respectively. The amount of sediment vented through reservoir outlets is essential for reservoir management; therefore, the simulated outflow concentration is crucial. Since the numerical model credibility based on comparing outflow concentration has been validated in the flume data, the simulated outflow concentrations over time through the desilting tunnel, the bottom outlet, and the spillway are plotted in Fig. 5(b). As shown in Fig. 5(b), it takes 18 hrs. for the front of the turbidity current to arrive at the bottom outlet, similar to the corresponding model prediction. It takes 36 hrs. for the current to arrive at the desilting tunnel by model prediction. The current reaches the spillway at 51 hrs., while the corresponding model prediction was 50 hrs., a difference of about 2%. The arrival time could be identified by the outflow sediment concentration, which presented an abrupt rising tendency of records up to 19,415 ppm for the bottom outlet; the concentration value continuously rose and reached the peak outflow concentration of 163,695 ppm. Whereas for the desilting tunnel, the abrupt rise of 42,416 ppm outflow concentration was observed at the timing while its gate was opened, reaching the peak concentration of 108,970 ppm. The measured peak outflows for the bottom

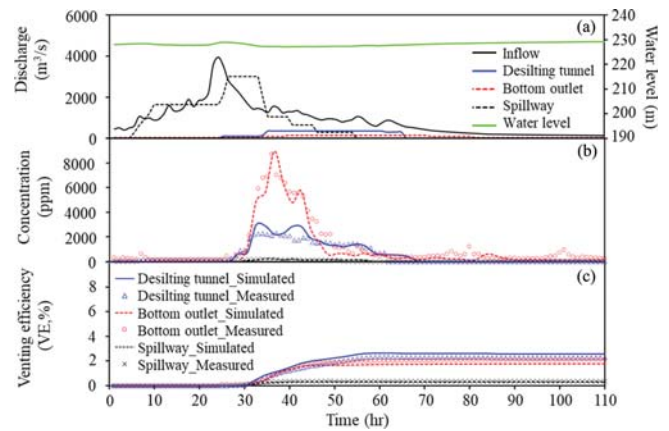


**Fig. 6.** In the Typhoon Lupit Event, the Hydrographs of: (a) Discharge and Water Level, (b) Simulated and Measured Concentration, (c) Simulated and Measured Venting Efficiency Through Various Outlets

outlet and desilting tunnel are 142,575 ppm and 96,048 ppm, respectively, with a difference of 14.81% and 13.5% from the simulated results. Due to the elevation of each outlet entrance, the outflow concentration at the bottom outlet has the highest value among the three outlets, whereas the spillway has the lowest one.

One of the essential variables for reservoir management during a flood event is the venting efficiency (VE) which can be calculated using an expression developed by Morris and Fan (2009) given as

$$VE = \left( \sum_{i=0}^T C_{oi} Q_{oi} \right) / Q_{ST} \quad (8)$$

where  $C_{oi}$  is the sediment concentrations of outflow, and  $Q_{oi}$  is the outflow discharges at time  $i$ , respectively;  $T$  is the duration of the flood event;  $Q_{ST}$  is the total inflow sediment yield. The VE value indicates the ratio of sediment discharge venting through the outlet to the inflow sediment discharge. In practice, the timing and arrangement of outlet gate opening significantly impact venting efficiency. Fig. 5(c) shows the cumulative VE through each outlet; the VE values of the desilting tunnel are the highest. Although sediment concentrations at the bottom outlet are far higher than those at the spillway, the outflow discharges of the spillway are larger than those of the bottom outlet while the spillway is opened.

The measured and the simulated total venting efficiency are 35.78% and 38.02%, respectively, with a difference of 3.88%. Through the desilting tunnel, the measured and simulated venting efficiencies are 21.90% and 22.78%, respectively, with a difference of about 4.02%. Through the bottom outlet, the measured and simulated venting efficiencies are 5.78% and 6.22%, respectively, with a difference of about 7.61%. Lastly, through the spillway, the measured and simulated venting efficiencies are 8.10% and 9.02%, respectively, with a difference of about 11.36%. Simulated results show consistency with the measured result. Hence, proving that the numerical model is capable of predicting turbidity current venting phenomena.

### 4.3 Turbidity Current Simulation using Field Data of Typhoon Lupit

In August 2021, Typhoon Lupit skirted the east coast of China as it moved into the Taiwan Strait. Approximately a total of 776 mm of rainfall was dropped in the Zengwen watershed. After Typhoon Lupit, a bathymetric survey was conducted, and the elevation of the reservoir bed in front of the dam was found to be higher than that of the bottom outlet, as seen in Fig. 1. With regular desilting operations through the outlets in typhoon flood events, both the bottom outlet and the power plant intake have still functioned well. The numerical model is applied to simulate the turbidity current generated during typhoon floods using field data of Typhoon Lupit acquired from the Southern Region Water Resources Office (Southern Region Water Resources Office, 2021c).

The hydrographs of the inflow discharge and the inflow sediment concentration were set as boundary conditions for the inlet, as shown in Fig. 6(a). A comparison of the measured and simulated outflow concentration hydrographs at the desilting tunnel, bottom outlet, and spillway is presented in Fig. 6(b). As shown in Fig. 6(b), the turbidity current reaches the bottom outlet at 28 hr., while the corresponding model prediction is 30 hrs., a difference of about 10.71%. In comparison, it takes 28 hrs. for the current to arrive at the desilting tunnel, while the corresponding model prediction was also 28 hrs., a difference of about 0%. The arrival time could be identified by the outflow sediment concentration, which presented an abrupt rising tendency of records up to 1143 ppm for the bottom outlet. The concentration value continuously rose and reached the peak outflow concentration of 8959 ppm. Whereas for the desilting tunnel, the abrupt rise of 632 ppm outflow concentration was observed, reaching the peak concentration of 2485 ppm. The measured peak outflows for the bottom outlet and desilting tunnel are 8719 ppm and 2258 ppm, respectively, with a difference of 2.75% and 10.05% from the simulated results.

The measured and the simulated total venting efficiency are 4.75% and 4.48%, respectively, with a total difference of 5.68%. Through each outlet, the measured and simulated venting efficiency are as follows: 0.35% and 0.31%, respectively, for the spillway with a difference of 11.43%; for the bottom outlet, 2.14% and 1.79%, respectively, with a difference of 16.36%; for desilting tunnel 2.27% and 2.37% respectively with a difference of 4.41%. Fig. 6(c) shows the cumulative VE value of each outlet; similar to the simulation results of typhoon Morakot, the VE value of the desilting tunnel is the highest.

Simulated results show consistency with the measured result, verifying the model's capability to simulate turbidity currents generated in the reservoir during typhoon floods.

### 4.4 Influence of Integrated Sediment Management Technique of Sediment Dredging and Routing on Venting Efficiency of Reservoir Outlets

#### 4.4.1 Dredged Guiding Channel: Description and Analysis

Sediment deposition and reservoir storage depletion are the two

most pressing challenges in Taiwan. Different techniques, including sediment routing, sediment yield reduction, and sediment removal, may be implemented in reservoir watersheds to counteract reservoir sedimentation. In the Zengwen Reservoir, the dredging operation has been active since 2012; the dredging area is close to the dam, which is the most accessible for operation. The current dredging process involves two boats that operate round the clock, and the maximum dredging capacity is 10,000 m<sup>3</sup>/day/boat. The total dredged volume from 2012 until 2022 has reached 14.74 Mm<sup>3</sup>. As mentioned in the Introduction, the purpose of dredging is to increase the storage capacity lost to sediment deposition. However, in addition to sediment removal by dredging, this study attempts to route turbidity currents generated during typhoon events toward the reservoir outlets to reduce sediment settling inside the reservoir and improve a reservoir's storage capacity.

Among many globally tested techniques, the sediment routing techniques have proven the most effective in reducing reservoir sedimentation and maintaining sediment continuity similar to pre-dam conditions. Sediment routing is a concept that refers to a group of techniques that utilize time-wise variation in sediment discharge to manage flows during floods to avoid sediment trapping in the reservoir. Moreover, these existing techniques can be modified and combined with other approaches to build up an efficient and feasible method that can potentially tackle the presented challenge. Therefore, devising a sediment management strategy that performs effectively during typhoon events and dry seasons is crucial for maintaining the reservoir's functionality. Hence, this study attempts to test a technique involving dredging a guiding channel on the reservoir bed that can help guide and concentrate the turbidity currents generated during the flood events towards the reservoir outlets. According to previous studies, the turbidity current's front velocity determines the distance it will travel and the rate at which it reaches a certain point (Morris and Fan, 2009). Therefore, the dredged guiding channel aims to aid the movement of turbidity currents generated during flood occurrences with higher velocity and concentration, reducing sediment concentration dissipation before arriving at the outlets.

The flood event of the five-year return period was simulated to determine the route of the dredged guiding channel. The velocity contour generated (see Fig. 7(a)) for flood simulation aids us in deciding the length and alignment of the dredged channel. From Fig. 7(a), the thalweg representing the watercourse with the lowest elevation within a reservoir acts as a mainstream of a reservoir, along which higher velocity is observed. However, upon crossing the A-06 reservoir cross-section, a decrease in velocity can be seen. Similar behavior was seen in the study of Wu et al. (2021), in which the velocity beyond section A-07 started to decrease; hence, higher sediment deposition was observed. From cross-sections A-10 to A-08, the turbidity current takes a turn due to the alignment of the reservoir, and at such events as well, it could be seen that there was a slight decrease in the velocity (Fig. 7(a)). Due to the decline in the velocity, deposition chances are higher if the currents generated are short-lived.

As mentioned in Section 2, to decide the width of a dredged

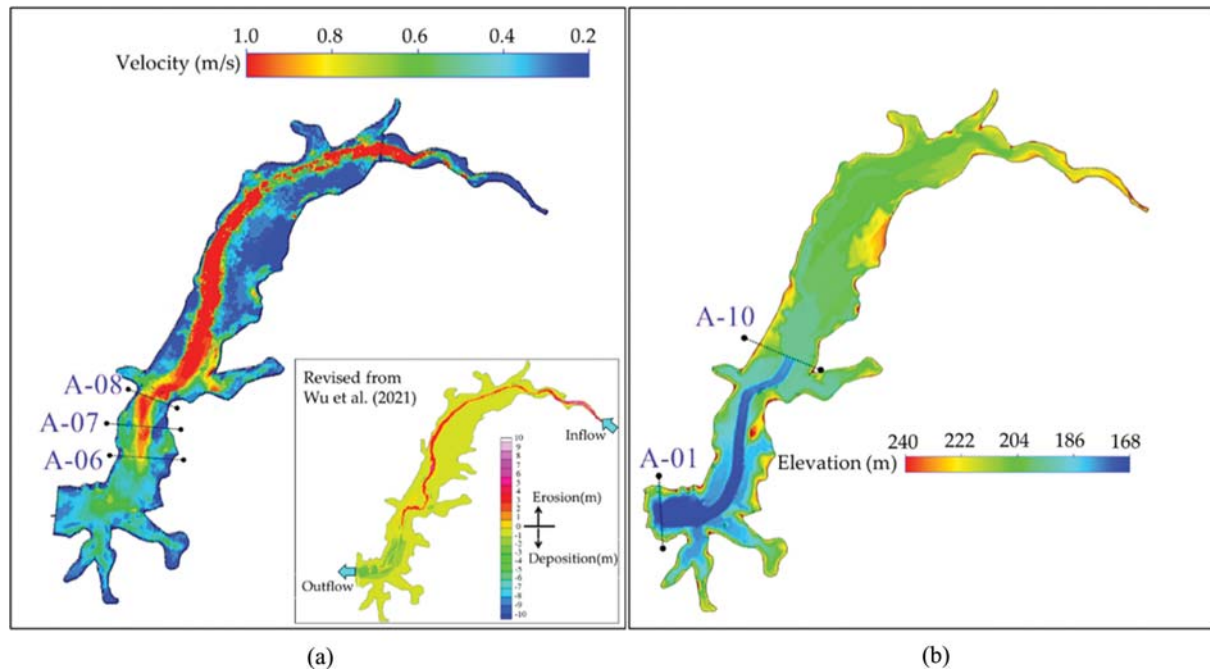


**Fig. 7.** Simulated Topography of Zengwen Reservoir Using Bathymetry Data of 2019: (a) Mainstream and Potential Dredged Guiding Channel Location, (b) With a Dredged Guiding Channel Extending from A-01 to A-10

channel, we have referred to the study reported by the Southern Region Water Resources Office (2021b), in which three field-workable widths of dredged channels of 50 m, 100 m, and 200 m were tested. According to the study findings, the venting efficiency is higher when the width is 200 m. Lastly, to decide the depth of the dredged channel, we referred to the geological drilling results report of the Zengwen reservoir (Southern Region Water Resources Office, 2021a). From the particle size analysis, the dominant presence of silt and clay and insignificant particle size variation along the depth of 15 m at BH-01 and BH-02 compared to BH-03 (closer to the dam) is observed; therefore, the depth of the dredged guiding channel needs to be within the feasible range of hydraulic dredging in the field. Moreover, the field-measured data reveals that the average movement velocity of turbidity current is less than one m/sec. Since we aim to direct the turbidity current towards the desilting tunnel (DT), hence based on the discharge capacity of DT being close to 1,000 m<sup>3</sup>/sec, the depth of the dredged guiding channel is designed at 5 m with the aim of turbidity current mainly traveling within the dredged channel. Therefore, considering all the factors mentioned above, the reservoir bed is modified by constructing a dredged channel extending from cross-sections A-1 to A-10 with a depth of 5 m and width of 200 m following the mainstream towards the desilting tunnel (Fig. 7(b)).

#### 4.4.2 Impact of Dredged Guiding Channel (DGC) on Venting Efficiency of Reservoir Outlet

To evaluate the functioning of the dredged guiding channel, we focused on its impact on the venting efficiency of reservoir outlets, especially on the desilting tunnel. Eight numerical simulations of

flood events of return periods 2, 5, 20, and 100 (i.e.,  $Q_2$ ,  $Q_5$ ,  $Q_{20}$ , and  $Q_{100}$ ) were conducted with and without the dredged channel. Flow discharge hydrographs of various return-period floods are based on the pattern of Typhoon Jangmi in September 2008, which had a single peak discharge close to that of the 5-year return-period flood. According to the hydrological analysis, the peak discharges of  $Q_2$ ,  $Q_5$ ,  $Q_{20}$ , and  $Q_{100}$  floods are 2,769 m<sup>3</sup>/sec, 4,431 m<sup>3</sup>/sec, 7,776 m<sup>3</sup>/sec, and 11,840 m<sup>3</sup>/sec, respectively. Based on the relationship of inflow discharges and sediment discharges (as shown in Fig. 4(b)), the peak sediment concentrations of 39,028 ppm, 54,135 ppm, 80,264 ppm, and 105,265 ppm are adopted for  $Q_2$ ,  $Q_5$ ,  $Q_{20}$ , and  $Q_{100}$  floods, respectively. Figs. 8(a) and 8(b) are inflow hydrographs for discharge and sediment concentration, respectively.

From the simulated results, the venting efficiency of the desilting tunnel, bottom outlet, and spillway is 16.6%, 2.09%, and 8.62%, respectively, under the flow condition of a 100-year return period which has an inflow peak discharge of 11,840 m<sup>3</sup>/sec similar to Typhoon Morakot (2009). However, considering the simulation results with the dredged guiding channel, the venting efficiency is 21.04%, 5.17%, and 11.22% for the desilting tunnel, bottom outlet, and spillway, respectively. This enhancement points towards the positive impact of the dredged guiding channel on venting efficiency across all outlets. As a result, the total venting efficiency with a dredged guiding channel increase by 10.1%. Further, it can be seen from Table 1 that the total venting efficiency rises by 3.26%, 2.31%, and 13.88% for flood events  $Q_2$ ,  $Q_5$ , and  $Q_{20}$ , respectively.

These figures highlight the substantial improvement in venting efficiency across varying flood magnitudes due to the introduction

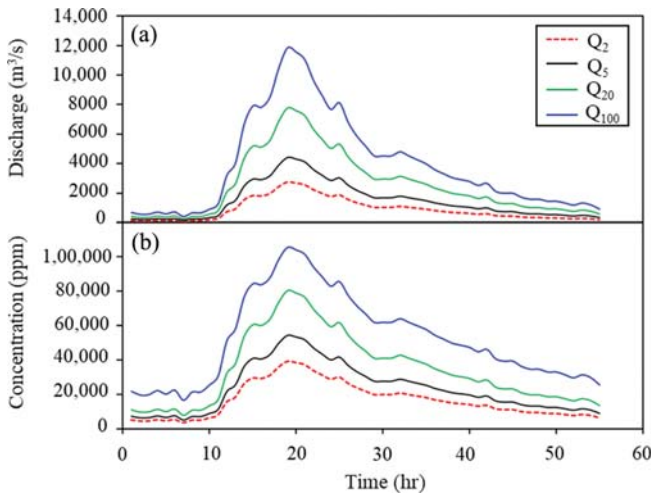


**Fig. 8.** Flow Hydrographs of: (a) Inflow Discharge, (b) Inflow Concentration of Four Flood Events Based on the Pattern of Typhoon Jangmi

of the dredged guiding channel. Significantly, the most notable improvement occurs at the desilting tunnel, with a nearly twofold increase in venting efficiency across all flood events when a dredged guiding channel is present. This improvement is critical in managing extreme flood events, mitigating flood risks and improve the overall safety and performance of hydraulic structures. Introducing a dredged guiding channel has an additional noteworthy impact on the flow dynamics within the system. It concentrates the turbidity current within the channel and leads to an increase in the flow velocity. This phenomenon significantly alters the behavior of sediment-laden water, optimizing its movement and channeling it more effectively through the system. As a result, the sediment transport is more contained and directed, reducing the dispersion and spread of sediments in unwanted areas while improving the overall flow dynamics within the designated channel moreover, this confinement and structuring of the turbidity current result in an increase in flow velocity. The streamlined channel allows for a more focused and accelerated movement of water and sediments, which, in turn, influences the venting efficiency of the outlets.

A scatter plot is used to display flood peak discharge and venting efficiency associated with and without the dredged guiding channel, which is further used for statistical regression

analysis to develop the relationship between venting efficiency and flood peak discharge for all reservoir outlets (Fig. 9). The figure can be used to predict the venting efficiency for different flood peaks and reservoir outlets.

Further, from Table 1, we see that the arrival time for  $Q_{100}$  was reduced from 13 hrs. to 9 hrs., showing turbidity current arrives earlier by 4 hrs. in the presence of DGC. A similar trend was observed for  $Q_{20}$ ,  $Q_5$ , and  $Q_2$ , in which the turbidity current reached 3, 3, and 2 hrs. earlier, respectively. As mentioned in Section 2, coordinating the gate opening to the arrival time is essential for optimum venting efficiency. Hence, the relationship using regression analysis is developed between turbidity current arrival time and peak discharge for both with and without DGC (see Fig. 9(e)), which will prove to be helpful in terms of the time of gate opening for maximum venting of turbidity currents and avoiding the formation of the muddy lake.

From a reservoir management standpoint, venting efficiency is a more crucial parameter. However, the amount of sediment trapped inside a reservoir provides an idea about the remaining storage capacity of a reservoir. It can be estimated by subtracting the total sediment outflow by venting operation from the total sediment yield. The sediment trapping efficiency (TE) is a commonly-used parameter to calculate the actual deposition volume and remaining storage capacity (Morris and Fan, 2009; Lewis et al., 2013; Tan et al., 2019). Hence, sediment trapping efficiency for the corresponding capacity-inflow ratio (CIR) has been calculated and plotted in Fig. 10. Fig. 10 also shows the relationship for observed data of annual base in the Zengwen reservoir, which presents an approximate similarity with the modified Brune curve referred to as the fitted TE curve, while the capacity inflow ratio was between 0.18 and 3. Focusing on the simulated results for DGC and without DGC, we see that the estimated TE values agree with a modified Brune curve trend, referred to as TE(I) curve shift-I and TE(II) curve shift-II respectively, for a capacity-inflow ratio of 0.6 – 2.8. However, the sediment trapping efficiency of a single event for four simulated capacity-inflow ratios can be seen to be lower than the observed data of the annual base. For example, for  $CIR \approx 0.6$ , the TE is 82.40% of the annual base, whereas, for simulated results without and with DGC, are 72.69% and 62.59%, respectively; similarly, for higher  $CIR \approx 1$ , the TE is 90.53% of annual base,

**Table 1.** Venting Efficiency of Each Reservoir Outlet with Inflow Conditions for Flood Return Periods of 2, 5, 20, and 100 Years

Flood return-period (year)	Inflow discharge volume (Mt)	Inflow sediment yield (Mt)	Inflow peak discharge ( $m^3/sec$ )	Inflow peak sediment concentration (ppm)	Turbidity current arrival time (hr.) (without/with dredged channel)	Outflow peak sediment concentration at DT (ppm) (without/with dredged channel)	Venting efficiency (%) (without/with dredged channel)				Total increase in VE (%)
							DT	BO	SW	Total	
$Q_2$	180.67	4.52	2769	39,028	26/24	1500/2500	3.62/5.82	0.08/0.13	0.001/1.01	3.70/6.96	3.26
$Q_5$	288.66	10.04	4431	54,135	20/17	2000/5000	4.83/13.50	0.24/1.35	0.01/1.20	9.10/11.41	2.31
$Q_{20}$	507.38	26.12	7776	80,264	15/12	9000/16,000	8.65/15.87	1.28/4.17	2.53/6.30	12.46/26.34	13.88
$Q_{100}$	772.55	56.39	11,840	1,05,265	13/9	56,000/78,000	16.6/21.04	2.09/5.17	8.62/11.22	27.31/37.41	10.1

\*Note: DT (desilting tunnel), BO (bottom outlet), SW (spillway).

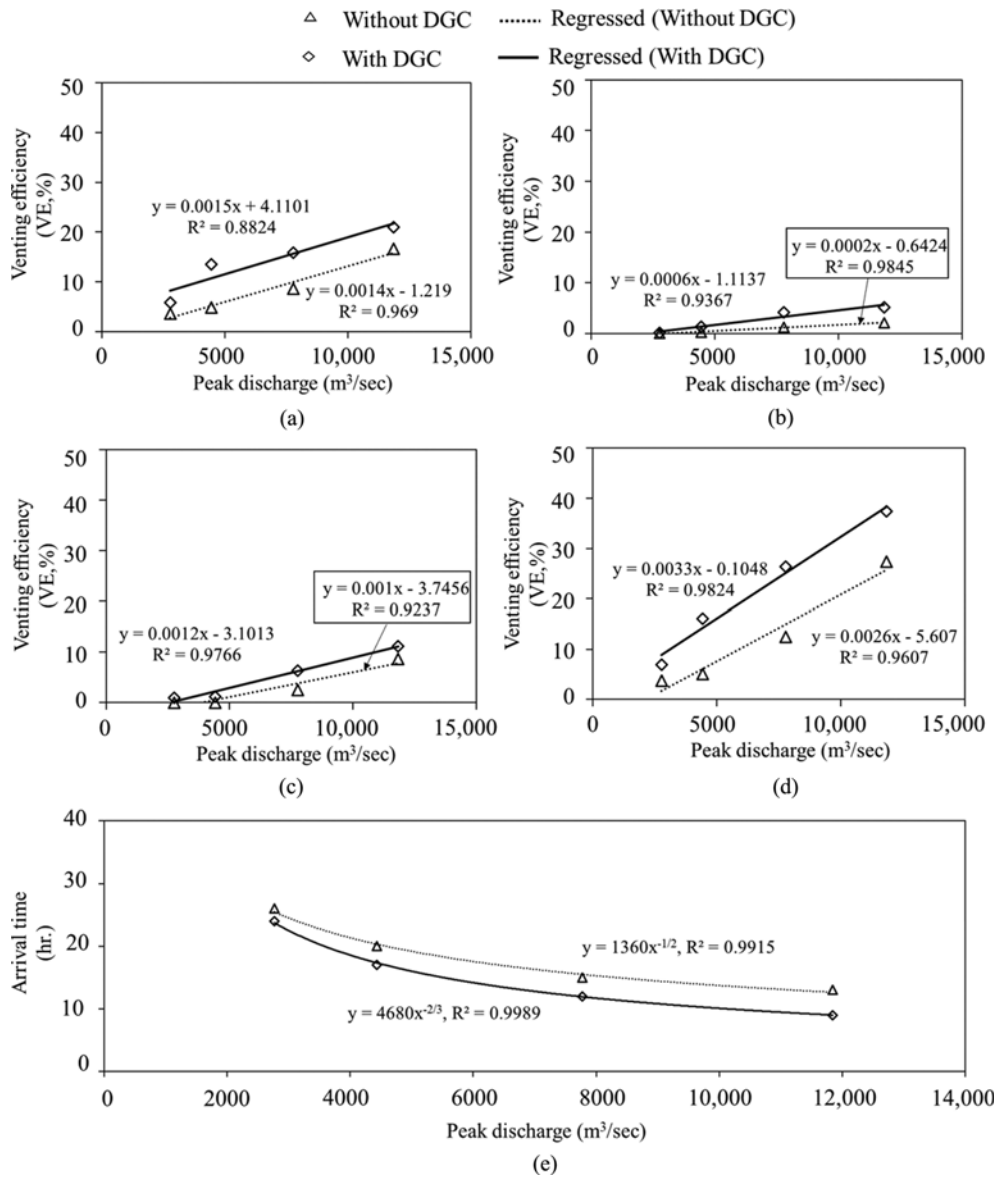


Fig. 9. Statistical Regression Analysis Used to Develop the Relationship between Venting Efficiency and Flood Peak Discharge for: (a) Desilting Tunnel, (b) Bottom Outlet, (c) Spillway, (d) Total VE, (e) Turbidity Current Arrival Time and Flood Peak Discharge

whereas, for simulated results without and with DGC are 82.54% and 73.66% respectively. Further trapping efficiency was estimated for previously simulated typhoon flood events of Morakot (2009) and Lupit (2021) and plotted in Fig. 10.

These typhoon floods are single events, and it can be seen that they fall towards the fitted TE curve. In addition, the TE(I) trend without DGC is higher than the TE(II) trend with the DGC condition. It also reveals that the TE of a higher hydrological event is lower than a small hydrological event. Hence, the findings prove that this study agrees with the tendency of the Brune curve (1953). Further, the relationship generated between TE(I) and CIR for simulated cases without DGC and TE(II) and CIR for simulation cases with DGC can aid in predicting the remaining storage capacity in the reservoir after a single typhoon flood event (see Fig. 10).

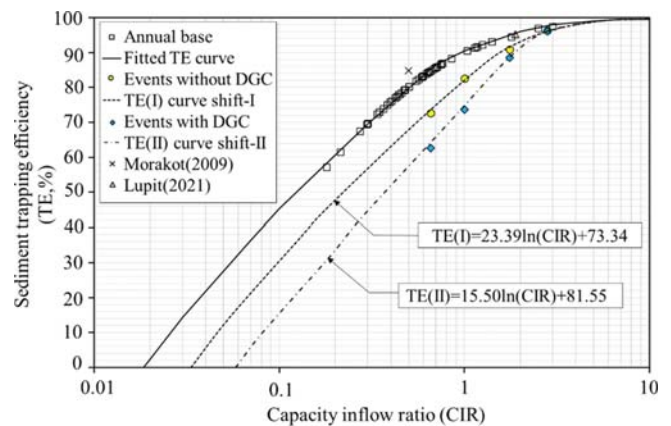


Fig. 10. Sediment TE as Related to Capacity Inflow Ratio Considering Annual Base and Sediment Management Strategy Adopted

## 5. Conclusions

Sediment management in the reservoirs is critical for sustainable water resources. This study investigates the effectiveness of an integrated reservoir management strategy of sediment dredging and routing by constructing a dredged guiding channel to maximize the venting of turbidity currents through reservoir outlets in the Zengwen reservoir. A 3D numerical model, ANSYS-CFX, is adopted to simulate turbidity currents generated in the reservoir during typhoon flood events. The flume data were used for mesh analysis and model calibration. The physical model data were used to verify the accuracy of simulated turbidity current arrival time and venting efficiency for bottom outlets. In addition, field data used were collected during Typhoon Lupit (2021) for model validation to corroborate that the calibrated parameters are unaffected by the scale effect between the laboratory test and the field.

To efficiently vent the turbidity current and reduce sediment deposition, the turbidity current must reach and sufficiently arrive at the reservoir outlets indicating that the velocity of a turbidity current must be sufficient enough to generate the turbulence required to maintain its sediment load in suspension. Therefore, turbidity current having a potential travel distance less than the length of the reservoir may not be successful in passing through the bottom outlets of the reservoirs. The study findings, however, show that the dredged guiding channel can concentrate turbidity currents and reduce the current dissipation. Further, the guiding channel also decreases the arrival time of the turbidity current at the dam, implying an increase in the velocity of the turbidity current. The effect of a dredged guiding channel on the functioning of reservoir outlets is evaluated in terms of venting efficiency; hence, when considering a guiding channel, the venting efficiency of reservoir outlets increases by a considerable amount. Since the guiding channel is directed towards the desilting tunnel, a significant increase in the venting efficiency of the desilting tunnel, varying with the flood return period, is observed. The study results can be used to estimate the sediment venting efficiency for each reservoir outlet and turbidity current arrival time for different peak discharges, thereby aiding in predicting trapping efficiency based on the Brune curve trend for different capacity inflow ratios for single flood events.

However, suppose a dredged guiding channel of dimensions other than those considered in this study is simulated. In that case, the simulated results of outflow sediment concentration, venting efficiency of each outlet, trapping efficiency inside the reservoir, and arrival time of the turbidity currents could be different. Nevertheless, feasibility in the field must be considered in the dredging operations. Therefore, this study has simulated the feasible dredging range, which can help tackle the reservoir sedimentation problem caused by typhoon floods.

## Acknowledgments

The authors acknowledge the Southern Region Water Resources Office, Taiwan, for providing the essential data for analysis and simulation. The authors also appreciate the Hydrotech Research

Institute of the National Taiwan University and National Chung Hsing University for providing computing facilities and technical support.

## Nomenclature

$a$	= Viscosity coefficient
$C_{oi}$	= Sediment concentrations of outflow at time $i$
$C_p$	= Sediment particle concentration
$d$	= Particle diameter
$g$	= Acceleration due to gravity
$G'$	= Buoyancy vector
$k$	= Turbulent kinetic energy
$m$	= Reynolds number (Re) dependent coefficient
$p'$	= Modified pressure
$Q_{oi}$	= Outflow discharges at time $i$
$Q_{ST}$	= Total inflow sediment yield
$T$	= Duration of the flood event
$u$	= Kinematic viscosity of water
$U_{i,j}$	= Velocity components
$VE$	= Venting efficiency
$w_f$	= Fall velocity of a sediment particle
$w_{ff}$	= Terminal fall velocity of a particle in clear water
$x_{i,j}$	= Cartesian coordinates
$\varepsilon$	= Turbulence dissipation rate
$\rho$	= Mixture density
$\rho_s$	= Particle density
$\sigma_p$	= Turbulent Prandtl number
$\rho_w$	= Water density
$\nu_{eff}$	= Effective viscosity
$\nu_t$	= Turbulence viscosity

## ORCID

Nafeela Imtiyaz  <https://orcid.org/0009-0002-2890-600X>

Fong-Zuo Lee  <https://orcid.org/0000-0003-0826-1435>

Gwo-Fong Lin  <https://orcid.org/0000-0003-3788-8085>

Jihn-Sung Lai  <https://orcid.org/0000-0003-4168-3090>

## References

- Amini A, Venuleo S, Chamoun S, De Cesare G, Schleiss AJ, Takhtemina F (2017) Investigation of venting turbidity currents in the Rudbar-Lorestan reservoir in Iran. *85<sup>th</sup> Annual Meeting of International Commission on Large Dams*, Prague, Czech Republic. 3-7 July 2017, <https://infoscience.epfl.ch/record/229961?ln=en>
- Annandale GW, Morris GL, Karki P (2016) Extending the life of reservoirs: Sustainable Sediment Management for Dams and Run-of-River Hydropower; Washington, DC, USA, DOI: 10.1596/978-1-4648-0838-8
- Brune GM (1953) Trap efficiency of reservoirs. *Transactions American Geophysical Union* 34:407-418, DOI: 10.1029/TR034i003p00407
- Camenen B (2007) Simple and general formula for the settling velocity of particles. *Journal of Hydraulic Engineering* 133:229-233, DOI: 10.1061/(ASCE)0733-9429(2007)133:2(229)
- Chamoun S, De Cesare G, Schleiss AJ (2017) Management of turbidity

- current venting in reservoirs under different bed slopes. *Journal of Environmental Management* 204:519-530, DOI: [10.1016/j.jenvman.2017.09.030](https://doi.org/10.1016/j.jenvman.2017.09.030)
- Chamoun S, De Cesare G, Schleiss AJ (2018) Influence of operational timing on the efficiency of venting turbidity currents. *Journal of Hydraulic Engineering*, 144, DOI: [10.1061/\(ASCE\)HY.1943-7900.0001508](https://doi.org/10.1061/(ASCE)HY.1943-7900.0001508)
- Chien N, Wan ZH (1999) The mechanics of sediment transport. *American Society of Civil Engineerig*, Reston, VA
- Dadson S, Hovius N, Chen H, Dade W, Hsieh ML, Willett S, Hu JC, Horng MJ, Chen MC, Stark C (2003) Links between Erosion, Runoff Variability and Seismicity in the Taiwan Orogen. *Nature* 426:648-651, DOI: [10.1038/nature02150](https://doi.org/10.1038/nature02150)
- De Cesare G, Boillat JL, Schleiss, AJ (2006) Circulation in stratified lakes due to flood-induced turbidity currents. *Journal of Environmental Engineering*, 132, DOI: [10.1061/\(ASCE\)0733-9372\(2006\)132:11\(1508\)](https://doi.org/10.1061/(ASCE)0733-9372(2006)132:11(1508))
- De Cesare G, Schleiss AJ, Hermann F (2001) Impact of turbidity currents on reservoir sedimentation. *Journal of Hydraulic Engineering*, 127, DOI: [10.1061/\(ASCE\)0733-9429\(2001\)127:1\(6\)](https://doi.org/10.1061/(ASCE)0733-9429(2001)127:1(6))
- Huang CC, Lai YG, Lai JS, Tan YC (2019) Field and numerical modeling study of turbidity current in shimen reservoir during typhoon events. *Journal of Hydraulic Engineering*, 145, DOI: [10.3390/w11071353](https://doi.org/10.3390/w11071353)
- Jodeau M, Chamoun S, Feng J, De Cesare G, Schleiss AJ (2018) Numerical Modeling of turbidity currents with Ansys CFX and Telemac 3D. *E3S Web of Conferences* 40:03014, DOI: [10.1051/e3sconf/20184003014](https://doi.org/10.1051/e3sconf/20184003014)
- Kondolf GM, Rémi L, Piégay H, Malavoi JR (2019) Dams and channel morphology. *Environmental Flow Assesment*, 143-161, DOI: [10.1002/9781119217374.ch8](https://doi.org/10.1002/9781119217374.ch8)
- Lai YG, Huang J, Wu K (2015) Reservoir turbidity current modeling with a two-dimensional layer-averaged model. *Journal of Hydraulic Engineering*, 141, DOI: [10.1061/\(ASCE\)HY.1943-7900.0001041](https://doi.org/10.1061/(ASCE)HY.1943-7900.0001041)
- Lee FZ (2013) Simulation and experiment of density current on venting efficiency and movement mechanism. Doctoral dissertation, National Taiwan University, Taipei, Taiwan, DOI: [10.6342/NTU.2013.00128](https://doi.org/10.6342/NTU.2013.00128) (in Chinese)
- Lee FZ, Lai JS, Sumi T (2022) Sediment management and downstream river impacts for sustainable water resources-case study of shihmen reservoir. *Water* 14:479, DOI: [10.3390/w14030479](https://doi.org/10.3390/w14030479)
- Lee FZ, Lai JS, Tan YC, Sung CC (2014) Turbid density current venting through reservoir outlets. *KSCE Journal of Civil Engineering* 18(2): 694-705, DOI: [10.1007/s12205-014-0275-y](https://doi.org/10.1007/s12205-014-0275-y)
- Lewis SE, Bainbridge ZT, Kuhnert PM, Sherman BS, Henderson B, Dougall C, Cooper M, Brodie JE (2013) Calculating sediment trapping efficiencies for reservoirs in tropical settings: A case study from the Burdekin Falls Dam, NE Australia. *Water Resources Research* 49:1017-1029, DOI: [10.1002/wrcr.20117](https://doi.org/10.1002/wrcr.20117)
- Mahmood K (1987) Reservoir sedimentation: Impact, extent, and mitigation. World Bank technical report 71, Washington, DC, USA, <http://documents.worldbank.org/curated/en/888541468762328736/Reservoir-sedimentation-impact-extent-and-mitigation>
- Marosi M, Ghomeshi M, Sarkardeh H (2015) Sedimentation control in the reservoirs by using an obstacle. *Sadhana*, 40, DOI: [10.1007/s12046-015-0333-2](https://doi.org/10.1007/s12046-015-0333-2)
- Morris GL, Fan J (2009) Reservoir sedimentation handbook: Design and management of dams, reservoirs, and Watersheds for Sustainable Use; McGraw-Hill, New York, NY, USA
- Oehy CD, Schleiss AJ (2007) Control of turbidity currents in reservoirs by solid and permeable obstacles. *Journal of Hydraulic Engineering-ASCE*, 133, DOI: [10.1061/\(ASCE\)0733-9429\(2007\)133:6\(637\)](https://doi.org/10.1061/(ASCE)0733-9429(2007)133:6(637))
- Richardson JF, Zaki WN (1954) The sedimentation of uniform spheres under conditions of viscous flow. *Chemical Engineering Science* 3:65-73, DOI: [10.1016/0009-2509\(54\)85015-9](https://doi.org/10.1016/0009-2509(54)85015-9)
- Sastre V, Loizeau JL, Greinert J, Naudts L, Arpagaus P, Anselmetti F, Wildi W (2010) Morphology and recent history of the rhone river delta in lake geneva (Switzerland). *Swiss Journal of Geosciences* 103:33-42, DOI: [10.1007/s00015-010-0006-4](https://doi.org/10.1007/s00015-010-0006-4)
- Schleiss AJ, Franca M, Juez C, De Cesare G (2016) Reservoir sedimentation. *Journal of Hydraulic Research* 54:1-20, DOI: [10.1080/00221686.2016.1225320](https://doi.org/10.1080/00221686.2016.1225320)
- Southern Region Water Resources Office (2021a) On-site geological drilling and soil test in Zengwen Reservoir. Tainan City, Taiwan: Southern Region Water Resources Office (in Chinese)
- Southern Region Water Resources Office (2021b) The feasibility study of catchment area diversion tunnels of Zengwen Reservoir. Tainan City, Taiwan: Southern Region Water Resources Office (in Chinese)
- Southern Region Water Resources Office (2021c) Maintenance of automatic monitoring system for sediment concentration and measurement data analysis of Zengwen Reservoir. Tainan City, Taipei, Taiwan: Southern Region Water Resources Office (in Chinese)
- Sung CC, Lai JS (2009) Establishment of sediment concentration observation system with monitoring, determination and analysis in Tsengwen reservoir (805), Hydrotech Research Institute, National Taiwan University, Taipei City, Taiwan (in Chinese)
- Tan G, Chen P, Deng J, Xu Q, Tang R, Feng Z, Yi R (2019) Review and improvement of conventional models for reservoir sediment trapping efficiency. *Heliyon* 5:e02458, DOI: [10.1016/j.heliyon.2019.e02458](https://doi.org/10.1016/j.heliyon.2019.e02458)
- Van Rijn LC (1987) Mathematical modelling of Morphological processes in the case of Suspended Sediment Transport. Doctoral dissertation, Delft Tech. Univ., Delft, The Netherlands
- Wang HW, Kondolf M, Tullos D, Kuo WC (2018) Sediment Management in Taiwan's Reservoirs and Barriers to Implementation. *Water* 10: 1034, DOI: [10.3390/w10081034](https://doi.org/10.3390/w10081034)
- Water Resources Planning Institute (2018) The feasibility study of catchment area diversion tunnels of Zengwen Reservoir physical model experiment on the desilting tunnel of Zengwen Reservoir. Taichung City, Taiwan (in Chinese)
- Wisser D, Frolking S, Hagen S, Bierkens MFP (2013) Beyond peak reservoir storage? A global estimate of declining water storage capacity in large reservoirs. *Water Resources Research* 49:5732-5739, DOI: [10.1002/wrcr.20452](https://doi.org/10.1002/wrcr.20452)
- Wu CW, Chou Frederick NF, Lee FZ (2021) Minimizing the impact of vacating instream storage of a multi-reservoir system: A trade-off study of water supply and empty flushing. *Hydrology and Earth System Sciences* 25:2063-2087, DOI: [10.5194/hess-25-2063-2021](https://doi.org/10.5194/hess-25-2063-2021)
- Zhiyao S, Wu T, Xu F, Li R (2008) A simple formula for predicting settling velocity of sediment particles. *Water Science and Engineering* 1(1): 37-43, DOI: [10.1016/S1674-2370\(15\)30017-X](https://doi.org/10.1016/S1674-2370(15)30017-X)